



HAL
open science

Termination impedance of open-ended cylindrical tubes at high sound pressure level

Merouane Atig, Jean-Pierre Dalmont, Joël Gilbert

► **To cite this version:**

Merouane Atig, Jean-Pierre Dalmont, Joël Gilbert. Termination impedance of open-ended cylindrical tubes at high sound pressure level. *Comptes rendus de l'Académie des sciences. Série IIb, Mécanique*, 2004, 332 (4), pp.299-304. hal-00474983

HAL Id: hal-00474983

<https://hal.science/hal-00474983>

Submitted on 21 Apr 2010

HAL is a multi-disciplinary open access archive for the deposit and dissemination of scientific research documents, whether they are published or not. The documents may come from teaching and research institutions in France or abroad, or from public or private research centers.

L'archive ouverte pluridisciplinaire **HAL**, est destinée au dépôt et à la diffusion de documents scientifiques de niveau recherche, publiés ou non, émanant des établissements d'enseignement et de recherche français ou étrangers, des laboratoires publics ou privés.

Termination impedance of open-ended cylindrical tubes at high sound pressure level

Mérouane ATIG, Jean-Pierre DALMONT, Joël GILBERT

Laboratoire d'acoustique de l'université du Maine, UMR CNRS 6613, avenue Olivier Messiaen,
72085 Le Mans Cedex 9, France
E-mail: merouane.atig@univ-lemans.fr

(Reçu le jour mois année, accepté après révision le jour mois année)

Abstract. The study deals with nonlinear acoustical effects localised at the open-end of a cylindrical tube. The termination impedance is measured using a two microphone method. Due to the separation of the acoustic flow at the pipe end, the real part of the termination impedance depends on the volume velocity at the open end. It is shown that the radius of curvature of the edges of the open end of the tube has a crucial influence on the amplitude of the nonlinear losses. Several regimes are shown for the low radii of curvature. © 2003 Académie des sciences/Éditions scientifiques et médicales Elsevier SAS

acoustics / wave guide / radiation impedance / nonlinearity

Impédance terminale d'un tuyau cylindrique ouvert à fort niveau sonore

Résumé. L'étude porte sur les effets acoustiques non-linéaires localisés à la sortie d'un tube cylindrique. Des mesures de l'impédance terminale réalisées à l'aide d'une méthode à deux microphones montrent que les pertes - partie réelle de l'impédance terminale - augmentent avec la vitesse moyenne en sortie de tube. L'importance de ces pertes dépend fortement du rayon de courbure des bords intérieurs à la sortie de tube. Les pertes peuvent être interprétées comme la conséquence de la séparation de l'écoulement acoustique en sortie de tube. Pour les faibles rayons de courbure, plusieurs régimes sont mis en évidence. © 2003 Académie des sciences/Éditions scientifiques et médicales Elsevier SAS

acoustique / guide d'onde / impédance de rayonnement / non-linéaire

1. Introduction

In a tube, when the sound pressure level is high, propagative nonlinear phenomena such as acoustic streaming or distortion of an acoustic wave [1] can appear. Beside these cumulative effects, there are localised nonlinear effects on geometrical discontinuities such as the open end of the tube for example.

These localised nonlinear effects are known for a long time in the case of an orifice. In 1935, Sivian [2] studied the nonlinear behaviour of the acoustic resistance of an orifice. Ingard & Labate [3] presented

Note présentée par First name NAME

S1620-7742(01)0????-?/FLA

© 2003 Académie des sciences/Éditions scientifiques et médicales Elsevier SAS. Tous droits réservés.

visualisations of the flow field around an orifice subjected to high-intensity sound. By measuring simultaneously sound pressure and flow velocity in an orifice, Ingard & Ising [4] concluded that the orifice resistance is proportionnal to the acoustic velocity for high sound amplitude. More recently, Disselhorst & Van Wijngaarden [5] observed the same behavior at the open end of a tube. As for an orifice, the real part of the termination impedance depends on the source sound level and increases with the acoustic velocity at the open end. Moreover, the open end geometry is crucial in this phenomenon. Peters et al. [6] studied the losses at an open end using different geometries such as a sharp edge, an unflanged pipe with thick walls or a circular horn.

The aim of the present study is to investigate experimentally the influence of the pipe termination geometries, and especially the role of the radius of curvature of the terminations, on the termination impedance. In the next section, the existing theoretical results for the termination impedance are presented for the linear and the nonlinear case. In section 3. the experimental setup is described. Finally, the results of the measurements for high sound amplitude are presented and discussed in section 4. followed by a conclusion.

2. Theoretical results

In linear acoustics, the termination impedance of a tube is called radiation impedance. The acoustic radiation impedance of a tube is a quantity defined as $Z_r = p/U$ where p and U are respectively the acoustical pressure and the acoustical volume velocity at the open end of a tube. The expression of the linear radiation impedance Z_r in the low frequency approximation is given by Levine & Schwinger [7] for an unflanged pipe, Nomura et al. [8] for a pipe with an infinite flange :

$$\frac{Z_r}{Z_c} = \begin{cases} \frac{1}{4}(ka)^2 + jk\delta_0 & \text{unflanged pipe, } \delta_0 = 0.6133a \\ \frac{1}{2}(ka)^2 + jk\delta_\infty & \text{infinitely flanged pipe, } \delta_\infty = 0.8216a \end{cases} \quad (1)$$

where $Z_c = \rho_0 c_0 / S$ is the characteristic impedance with ρ_0 air density, c_0 speed of sound and S surface area of the tube, $k = \omega / c_0$ is the wave number ω being the angular frequency, a is the tube radius, δ_0 and δ_∞ the so-called end length correction for an unflanged tube and a flanged tube respectively. The real part of the radiation impedance represents the radiation loss and the imaginary part represents the inertia.

When the amplitude of the acoustical velocity is high enough, nonlinear effects appear at the end of an open pipe : there is separation of the acoustic flow at the pipe end and formation of vortices. This effect causes an increase of energy losses at the open end implying an increase in the real part of the termination impedance. Harmonic distortion can also appear. Strictly speaking, impedance is defined for linear systems so, in the following, termination impedance Z_{end} is defined as the ratio between pressure and velocity at the open end for the fundamental harmonic (first harmonic approximation). The acoustical parameter chosen to characterise the phenomena are the acoustic Strouhal number based on the tube radius $St = \omega a / \hat{u}$ and the acoustic Mach number $M = \hat{u} / c_0$, where \hat{u} is the amplitude of the acoustic velocity averaged over the cross sectional area of the open end. Disselhorst & Van Wijngaarden [5] and Peters et al. [6][9] modelled the nonlinear behavior of an open pipe. The results found by Disselhorst & Van Wijngaarden [5] for high Strouhal numbers (equation 7.11) can be thought of as an additional term Z_{nl} to the radiation impedance so that $Z_{end} = Z_r + Z_{nl}$:

$$\frac{Z_{nl}}{Z_c} = \beta . M . St^{\frac{1}{3}}. \quad (2)$$

The parameter β is determined by means of numerical simulation. Disselhorst & Van Wijngaarden [5] found values between 0.6 and 1.0 and Peters & Hirschberg [9] found a value of 0.2.

For low Strouhal numbers, i.e. high amplitude of the acoustic velocity, Peters et al. [6] (equation 5.26) propose the use of a quasi-steady theory. During half a period, the acoustic velocity is oriented out of the tube and a jet-like outflow is assumed. During the second half period, the acoustic velocity is oriented into the tube and there is formation of a vena-contracta type of inflow. The parameter c_d , which characterises

Termination impedance of open-ended cylindrical tubes at high sound pressure level

the vena contracta for different pipe end geometries, can be introduced. The additional term Z_{nl} is then given by

$$\frac{Z_{nl}}{Z_c} = \frac{2c_d}{3\pi} M. \quad (3)$$

c_d is equal to 2 for a thin-walled unflanged pipe and equal to 13/9 for a flanged pipe [10].

3. Setup and experimental procedure

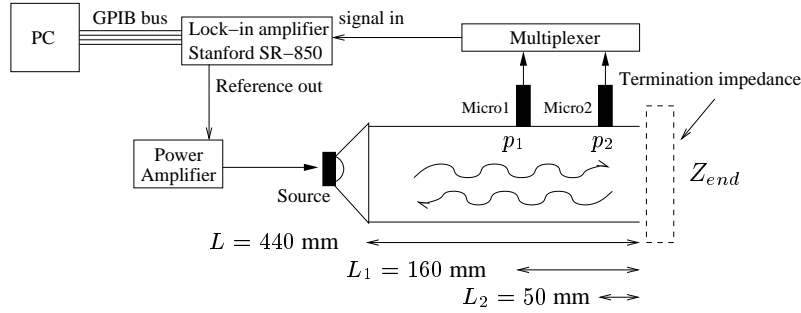


Figure 1: Experimental setup

The experimental setup is drawn schematically in figure 1. The measurements have been carried out using a copper tube of inner radius $a = 8$ mm. The wall thickness of the tube is $d = 1$ mm. The fundamental harmonic of the acoustic pressure in the pipe is measured by synchronous detection using acceleration compensated piezo-electrical gauges (PCB model 106B). The sound source is a compression driver JBL model 2446H and is located at one end of the tube. Five different terminations can be mounted at the open end of the tube (figure 2). The terminations geometries are of two types and have been chosen to influence the separation of the acoustic flow at the pipe end :

- the first type of termination has rounded edges which are defined by their radius of curvature r and presents a little flange (wall thickness $d = 4.5$ mm). Four radii of curvature have been chosen : $r < 0.01$, $r = 0.3$, 1 and 4 mm.
- the second type of termination, which tries to approximate the unflanged pipe termination with thin wall, has a sharp edge with a bevel angle of 20° and corresponds to the case studied experimentally by Disselhost & Van Wijngaarden [5] and Peters et al. [6]

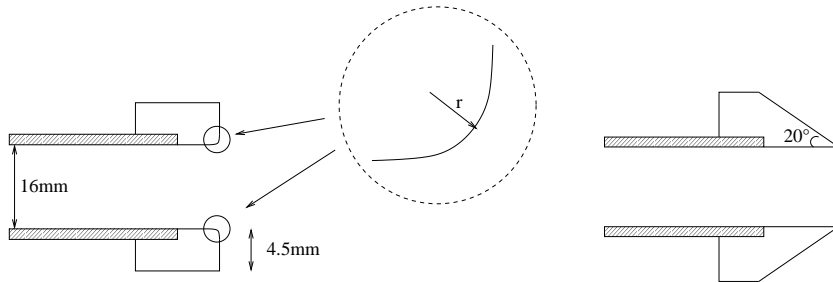


Figure 2: The two types of pipe termination geometry. **left)** Tube with rounded edges defined by a radius of curvature r , four radii of curvature have been chosen : $r < 0.01$, $r = 0.3$, 1 and 4 mm. **right)** Tube with a sharp edge defined by a bevel angle of 20° .

This setup is placed in the middle of an anechoic room. It is possible to measure by means of a two microphone method the pressures and velocities on any section of the tube assuming the plane wave hypothesis (for references about this method and errors analysis, see for example Bodén & Åbom [11]). With $H_{12} = p_2/p_1$ ratio of pressures measured on two points of the tube, the acoustic velocity at the open end is given by :

$$u = j \frac{p_1}{Z_c} \frac{H_{12} \cos(kL_1) - \cos(kL_2)}{\sin k(L_1 - L_2)}, \quad (4)$$

where L_i ($i = 1, 2$) is the distance between the microphone i and the exit of the pipe. The termination impedance is :

$$\frac{Z_{end}}{Z_c} = j \frac{H_{12} \sin(kL_1) - \sin(kL_2)}{\cos(kL_2) - H_{12} \cos(kL_1)}. \quad (5)$$

The calibration of the microphones is done by means of a Bruel & Kjaer microphone mounted flush in a wall which closes the tube. The calibration data shows that the two microphones have the same sensitivity (less than 1% of deviation) and are identical in phase (difference lower than 1°). The measurement of a closed pipe allows us to estimate the accuracy of the experiment. The error on $\text{Re}(Z_{end})$ is estimated to be less than $2 \cdot 10^{-3} Z_c$ and the one on δ is estimated to be less than $0.03a$.

A frequency sweep is made with the termination of radius of curvature $r = 4$ mm for a low excitation amplitude. It is verified that the experimental results fit in between the two limit cases of the unflanged [7] and the infinitely flanged pipe [8] as shown on figure 3. The resonance frequency of the whole system is found to be $f = 380$ Hz which corresponds to $ka \simeq 0.056$. The frequency of the source signal is then set to this value in order to obtain the maximum velocity at the open end. The acoustical Strouhal number is varied between 0.8 and 200 by changing the source level.

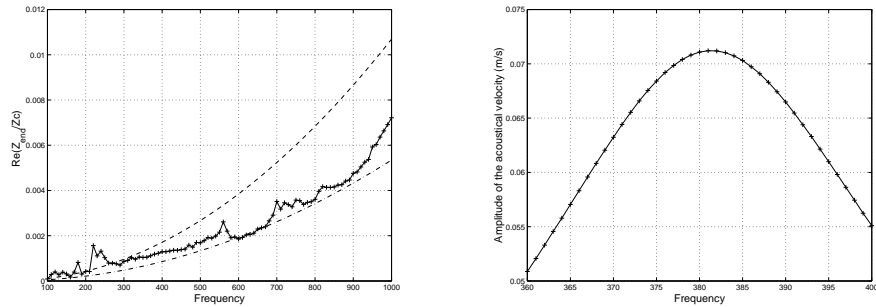


Figure 3: **left**) Real part of termination impedance as a function of the frequency at very low amplitude. (---) theories for flanged (upper) and unflanged pipe (lower). **right**) Amplitude of the acoustical velocity at the open end around resonance frequency.

4. Experimental results

Figure 4. compares the experimental data for the real part and for the imaginary part (represented by the length correction) of the termination impedance for the five terminations described in section 3. Theoretical predictions presented in section 2. are plotted on the same figure.

The experimental data corresponding to the termination $r = 4$ mm show that the real part of the termination impedance behaves approximately as the linear model given by equation 1 for acoustic velocities under 10 m/s. For higher acoustic velocities, nonlinear losses appear implying a slight increase in the real part of the termination impedance. For a termination with a smaller radius of curvature (termination $r = 1$ mm), the acoustic velocity threshold v_{nl} below which the acoustic resistance (real part of the termination impedance) behaves as the radiation impedance is around 7 m/s. If the radius of curvature is reduced again

Termination impedance of open-ended cylindrical tubes at high sound pressure level

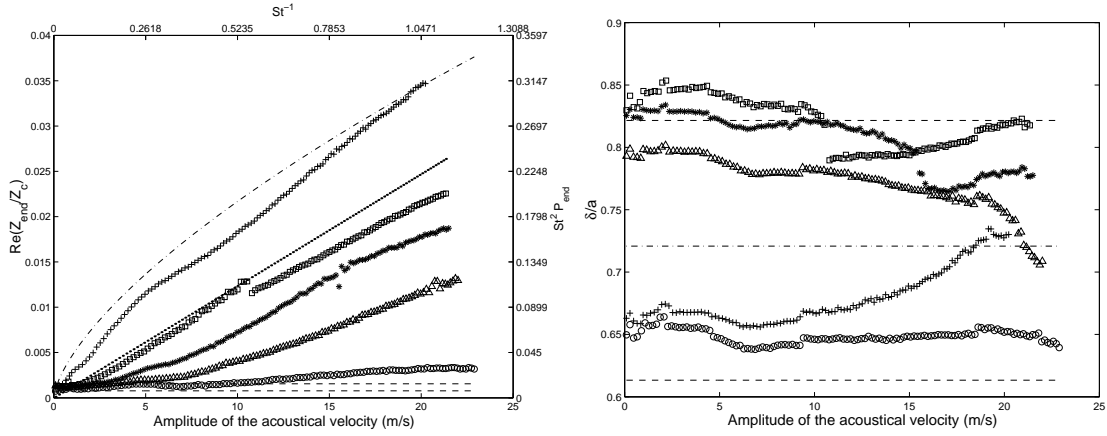


Figure 4: **left**) Real part of the termination impedance as a function of the amplitude of the acoustical velocity at the open end for the five different terminations. (+) sharp edge ; (\square) $r < 0.01$ mm ; (*) $r = 0.3$ mm ; (\triangle) $r = 1$ mm ; (\circ) $r = 4$ mm ; $(-\cdot-\cdot)$ eq.2 with $\beta = 0.6$; $(\cdot\cdot\cdot)$ eq.3 with $c_d = 2$; $(---)$ eq.1 for flanged (upper) and unflanged pipe (lower). A second scale, used by Disselhorst & Van Wijngaarden [5], representing the adimensioned power $St^2 P_{\text{end}} = \frac{1}{2}(MSt)^{-1} \text{Re}(Z_{\text{end}}/Z_c)$ in function of inverse Strouhal number is also indicated.

right) Length correction of the tube for five different terminations. (+) sharp edge ; (\square) $r < 0.01$ mm ; (*) $r = 0.3$ mm ; (\triangle) $r = 1$ mm ; (\circ) $r = 4$ mm ; $(---)$ theories for flanged (upper) and unflanged pipe (lower) ; $(-\cdot-\cdot)$ semi-empirical value [12] corresponding to the actual flange.

(terminations $r = 0.3$ mm and $r < 0.01$ mm), v_{nl} diminishes. The smaller the radius of curvature, the lower the threshold v_{nl} . The sharp edge termination experimental data show that the threshold appears to be much lower (less than 0.5 m/s). For velocities higher than v_{nl} , nonlinear losses increase linearly with the acoustical velocity as observed by Disselhorst & Van Wijngaarden [5]. Moreover, the rate of increase of these losses also depend on the radius of curvature. When the radius of curvature decreases, the slope of the nonlinear losses increases.

The experimental data for the termination $r < 0.01$ mm fit with the equation 3 ($c_d = 2$) for velocities up to 10.6 m/s. Then, a discontinuity in the acoustic resistance occurs. The phase of the pressure signal measured on the microphones for this velocity is unstable. This was first suspected to be a measurement set-up artefact but the phenomenon is reproducible. It has been observed with two different sources, different tube lengths and several frequencies. The same kind of discontinuity can be observed to a lesser extent with the terminations $r = 0.3$ mm and $r = 1$ mm. Notice that Peters et al. [6] have observed something similar they called “a strong dip in the acoustic power absorption” at a value of the acoustical Strouhal number close to $St = 5$. They indicate that “for this Strouhal number vortices formed at the sharp edge of the pipe end travel during one period of the acoustic field over a distance of the order of the wall thickness d ”. Figure 4. shows that the discontinuity corresponds in our experiment to St values between 1 and 2 depending on the termination. Increasing the flange of the tube using a collar decreases slightly the Strouhal number at which the discontinuities occur, typically for the termination $r < 0.01$ mm $\Delta St < 0.1$. The discontinuity on the measured termination impedance could be the signature of a transition between two different regimes of oscillation. J. Peube [13], in her experimental study of the open end of a pipe, observed experimentally different behaviours of the acoustical flow and in particular the appearance of turbulence near the edges of the tube for a particular value of a Reynolds number based on the thickness of the viscous boundary layer $A/2\pi\sqrt{f/\nu} \simeq 22$ with A amplitude of the acoustic displacement and ν

kinematic viscosity. In our experiment, we obtain values between 19 and 39 depending on the termination. Complementary measurements using visualisations techniques would be needed to analyse what happens around the discontinuities.

The experimental data for the so-called length correction are presented in figure 4.. The theoretical values from equation 1 and a semi-empirical value given by Dalmont et al. [12] for a 4.5 mm circular flange are also presented. All the experimental data are within the limits of the existing theory. For acoustic velocities under 10 m/s, all the terminations have the same behaviour. Then, the length correction for the termination $r = 4$ mm doesn't change with increasing acoustic velocity whereas the other rounded termination length correction seems to slightly decrease with the acoustic velocity. The sharp edge length correction increases with the acoustic velocity for acoustic velocities over 10 m/s. Discontinuities can be observed both in the real and imaginary part of the termination impedance for the same excitation level. Small discontinuities can also be observed on the imaginary part (for acoustical velocities of 9, 18 and 21 m/s) but these are lower than the measurement accuracy and are probably not relevant.

5. Conclusion

The experimental data presented here show the importance of the geometry of the open end of a tube on the behaviour of the real part of the termination impedance. For high acoustic velocities, the radiation losses are linked to the curve radius of the edges of the open end of a tube. The smaller the radius of curvature, the larger the nonlinear losses. On the contrary, the length correction of the tube do not depend significantly on the acoustic velocity. Flow visualisations such as those done by Rockliff [14] or Duffourd et al. [15] using particle image velocimetry (PIV) could allow to understand what happens at the discontinuity.

Acknowledgements. The authors would like to thank S. Collin for the machining of the terminations and D. Skulina for english corrections.

References

- [1] O.V. Rudenko and S.I. Soluyan. *Theoretical foundations of nonlinear acoustics*. Consultant Bureau, 1977.
- [2] L.J. Sivian. Acoustic impedance of small orifices. *J. Acoust. Soc. Am.*, 7:94–101, 1935.
- [3] U. Ingard and S. Labate. Acoustic circulation effects and the nonlinear impedance of orifices. *J. Acoust. Soc. Am.*, 22(2):211–218, 1950.
- [4] U. Ingard and H. Ising. Acoustic nonlinearity of an orifice. *J. Acoust. Soc. Am.*, 42(1):6–17, 1967.
- [5] J.H.M. Disselhorst and L. Van Wijngaarden. Flow in the exit of open pipes during acoustic resonance. *J. Fluid Mech.*, 99(2):293–319, 1980.
- [6] M.C.A.M. Peters, A. Hirschberg, A.J. Reijnen, and A.P.J. Wijnands. Damping and reflection coefficient measurements for an open pipe at low Mach and low Helmholtz numbers. *J. Fluid Mech.*, 256:499–534, 1993.
- [7] H. Levine and J. Schwinger. On the radiation of sound from an unflanged circular pipe. *Phys. Rev.*, 73(4):383–406, 1948.
- [8] Y. Nomura, I. Yamamura, and S. Inawashiro. On the acoustic radiation from a flanged circular pipe. *J. Phys. Soc. Jap.*, 15(3), 1960.
- [9] M.C.A.M. Peters and A. Hirschberg. Acoustically induced periodic vortex shedding at sharp edged open channel ends: simple vortex models. *J. Sound Vib.*, 161(2):281–299, 1993.
- [10] J.H.M. Disselhorst. *Acoustic resonance in open tubes*. PhD thesis, Twente University of Technology, 1978.
- [11] M. Åbom H. Bodén. Influence of errors on the two-microphone method for measuring acoustic properties in ducts. *J. Acoust. Soc. Am.*, 79(2):541–549, 1986.
- [12] J.-P. Dalmont, C.J. Nederveen, and N. Joly. Radiation impedance of tubes with different flanges: numerical and experimental investigations. *J. Sound Vib.*, 244(3):505–534, 2001.
- [13] J. Peube. Etude expérimentale du champ des vitesses à l'embouchure d'un tuyau sonore excité à de fortes amplitudes. *J. Phys. (Paris)*, 40:346–352, 1979.
- [14] D. Rockliff. *Application of particle image velocimetry to the measurement of non-linear effects generated by high-intensity acoustic fields*. PhD thesis, University of Edinburgh, 2002.
- [15] S. Duffourd, D. Marx, and P. Blanc-Benon. Détermination de la vitesse acoustique instantanée par PIV dans un stack thermoacoustique. In *Actes du 6e congrès d'acoustique*, pages 535–538, 2002.